

# Stochastic Gradient MCMC for Massive Geostatistical Data

Mohamed A. Abba

Department of Statistics, North Carolina State University

Brian J. Reich

Department of Statistics, North Carolina State University

Reetam Majumder

Southeast Climate Adaptation Science Center, North Carolina State University

Brandon Feng

Department of Statistics, North Carolina State University

June 5, 2024

## Abstract

Gaussian processes (GPs) are commonly used for prediction and inference for spatial data analyses. However, since estimation and prediction tasks have cubic time and quadratic memory complexity in number of locations, GPs are difficult to scale to large spatial datasets. The Vecchia approximation induces sparsity in the dependence structure and is one of several methods proposed to scale GP inference. Our work adds to the substantial research in this area by developing a stochastic gradient Markov chain Monte Carlo (SGMCMC) framework for efficient computation in GPs. At each step, the algorithm subsamples a minibatch of locations and subsequently updates process parameters through a Vecchia-approximated GP likelihood. Since the Vecchia-approximated GP has a time complexity that is linear in the number of locations, this results in scalable estimation in GPs. Through simulation studies, we demonstrate that SGMCMC is competitive with state-of-the-art scalable GP algorithms in terms of computational time and parameter estimation. An application of our method is also provided using the Argo dataset of ocean temperature measurements.

*Keywords:* Gaussian processes, SGMCMC, spatial data, Vecchia approximation, scalable inference.

# 1 Introduction

Gaussian process (GP) modeling is a powerful statistical and machine learning tool used to tackle a variety of tasks including regression, classification, and optimization. Within spatial statistics, in particular, GPs have become the primary tool for inference (Gelfand and Schliep, 2016). In spatial regression and classification problems, the response variable is assumed to have a spatially-correlated structure. GPs model this spatial dependence by specifying a form for the correlation between any two points in the spatial domain. In this paper we focus on the regression setting under the Matérn correlation with large amounts of data. Formally, GPs place a prior on the spatial process using a parameterized correlation function, which allows us to estimate *a posteriori* the parameters given the observed data.

One of the main advantages of GPs is their ability to provide predictions at unobserved locations along with uncertainty quantification. Spatial interpolation, commonly known as Kriging (Woodard, 2000), provides optimal predictions at unobserved sites based on the correlation between a given location and its observed neighbours (Cressie, 1988). However, handling large datasets with GPs poses computational challenges due to the cubic time complexity and quadratic memory requirements for the evaluation of the joint likelihood. This prohibitive computational cost mainly results from the evaluation of the covariance matrix and computing its inverse. Several methods have been proposed to address this issue and make GPs more scalable for large datasets. In this work, we combine stochastic gradient (SG) methods along with the Vecchia (Vecchia, 1988) approximation to develop an efficient algorithm for scalable Bayesian inference in massive spatial data settings. In the following section we review some of the main methods used to scale GPs (see Heaton et al., 2019, for a full survey), and briefly discuss applications of SG methods in correlated and dependent data settings.

## 1.1 Methods to handle large spatial datasets

The main computational bottleneck in GP regression is evaluating the inverse of the covariance matrix. To overcome this problem, a large body of literature has been proposed over the last decades, including but not limited to low rank approximations, covariance tapering, divide-and-conquer strategies, and Vecchia-type methods. Although these approaches differ significantly, they all tend to result in an amenable structure on the covariance or its inverse.

A low-rank approximation of the GP can be used to overcome the covariance inverse cost, (*e.g.*, Cressie and Johannesson (2008); Katzfuss and Cressie (2011); Kang et al. (2009)). Low-rank approximations project the spatial process on a low-dimensional space and use the low-rank representation as a surrogate to approximate the original process. Banerjee et al. (2008) used predictive process methods, where first a certain number of knots are placed in the spatial domain, then used as a conditioning set for the expectation of the original process. Fixed rank kriging (Cressie and Johannesson, 2008) approximates the original process using a small number of basis functions, which results in a precision matrix that can be obtained by inversion of a matrix with a much smaller dimension.

Instead of approximating the original process, one can impose fixed structures on the covariance or precision matrices directly. This method, also known as covariance tapering (Furrer et al., 2006; Kaufman et al., 2008), imposes a compact support on the correlation function, and hence correlation between a site and distant neighbours is shrunk to zero. This induces a sparse structure on the covariance that is leveraged to speed up the computation. Instead of imposing a structure on the covariance, Rue et al. (2009) directly impose a sparse structure on the precision matrix using a Gaussian Markov random field approximation to the true process.

Divide-and-conquer approaches have also been proposed to scale GPs inference. Barbian and Assunção (2017) and Guhaniyogi and Banerjee (2018) propose splitting the spatial domain in

subsets, performing the analysis in parallel on each subset, and then combining the results. This strategy distributes the workload into smaller parts. Another option is to divide the spatial region into independent sub-regions and perform the analysis on the whole dataset under this assumption (Sang et al., 2011). Unlike the former, the latter uses the whole dataset but reduces the computational cost using independence between subregions.

One of the earliest and most influential methods for scalable GPs is the Vecchia approximation (Vecchia, 1988; Stein et al., 2004). In the Vecchia framework, the full likelihood is factorized into a series of conditional distributions. This factorization is then simplified by reducing the conditioning sets to include a small number of neighbours, which in turn results in a sparse precision matrix. Guinness (2018) showed that Vecchia’s method is an accurate approximation to the true Gaussian process model in terms of the Kullback-Leibler divergence. This approach is also well suited for parallel computing due to the factorization of the likelihood. Recent works have built upon and extended the Vecchia approximation. Katzfuss and Guinness (2021) propose a generalization of the Vecchia’s framework and show that many existing approaches to Gaussian process approximation can be viewed as a special case of the extended method. Datta et al. (2016) proposed the nearest-neighbor Gaussian process as an extension of the Vecchia approximation, later, Finley et al. (2019) outline an efficient Markov Chain Monte Carlo (MCMC) algorithm for scalable full Bayesian inference using this method.

In general, all the aforementioned methods reduce the computational cost from cubic to linear in the number of observations. However, in the Bayesian framework we are mostly interested in posterior sampling through MCMC methods in order to get uncertainty estimates of the model parameters as well predictive credible intervals for certain locations. Typically, MCMC methods require thousands of iterations to accurately approximate the posterior distribution. Hence, even when the cost per iteration is linear, the total time can still be prohibitive. Recent work has there-

fore also focused on subsampling approaches for spatial data to reduce the computational cost associated with posterior sampling. Saha and Bradley (2023) have developed an efficient composite sampling scheme for posterior inference. Similarly, Heaton and Johnson (2023) use minibatches to approximate the complete conditional distribution of conjugate parameters, and provide an approximate Metropolis-Hastings (MH) acceptance probabilities for non-conjugate parameters. While Heaton and Johnson (2023) use a Vecchia approximation to define the minibatches, neither of these two works use any gradient information when drawing samples from the posterior, and are therefore fundamentally different from the gradient-based approach we will employ in our study.

## 1.2 Review of stochastic gradient methods

When dealing with large datasets, stochastic gradient (SG) methods (Robbins and Monro, 1951) have become the default choice in machine learning (Hardt et al., 2016). To avoid computing a costly gradient based on the full dataset, SG methods only require an unbiased and possibly noisy estimate using a subsample of the data. When the data is independent and identically distributed (*iid*) a proper scaling of the gradient based on a given subsample of the data yields an unbiased gradient estimate. The popularity and success of SG methods in optimization eventually lead to their adoption for scalable Bayesian inference (Nemeth and Fearnhead, 2021). Scalable SG Markov Chain Monte Carlo (SGMCMC) methods for posterior sampling in the *iid* setting have been proposed (Welling and Teh, 2011; Chen et al., 2015; Ma et al., 2015; Dubey et al., 2016; Baker et al., 2019). Convergence of SGMCMC methods has also received considerable attention. Under mild conditions, SGMCMC methods produce approximate samples from the posterior (Teh et al., 2016; Durmus and Moulines, 2017; Dalalyan and Karagulyan, 2019).

Although SG methods are widely used in the *iid* setting, their possible use in the correlated setting is still new. A naive application of SGMCMC methods in the correlated setting would

overlook critical dependencies in the data during subsampling. Moreover, the gradient estimate from the subsamples cannot be guaranteed to be unbiased. To the best of our knowledge, subsampling methods for spatial data that result in unbiased gradient estimates has not been addressed. Chen et al. (2020) studied the performance and theoretical guarantees for SG optimization for GP models. Although, the gradient based on a minibatch of the data leads to biased estimates of the full gradient of the log-likelihood, Chen et al. (2020) established convergence guarantees for recovering recovering noise variance and spatial process variance in the case of the exponential covariance function. In their work, the length scale parameter, which controls the degree of correlation between distinct points is assumed known, and no convergence result is provided. Recent works have considered other types of dependent data. In the case of network data, Li et al. (2016b) developed an SGMCMC algorithm for the mixed-member stochastic block models. Ma et al. (2017) leveraged the short-term dependencies in hidden Markov models to construct an estimate of the gradient with a controlled bias using non-overlapping subsequences of the data. This approach was extended to linear and non-linear state space models (Aicher et al., 2019, 2021).

SGMCMC methods can be divided in two main groups based on either Hamilton dynamics (Chen et al., 2014) or Langevin dynamics (Welling and Teh, 2011). In this work we use the Langevin dynamics (LD) method due to its lower number of hyperparameters, our approach can be extended to the Hamiltonian dynamics with minor modifications. We extend the SGLD method to the case of non-*iid* data using the Vecchia approximation and provide a method that takes account of the local curvature to improve convergence.

In the remainder of this paper, Section 2 discusses the Matérn Gaussian process model and the Vecchia approximation used to obtain unbiased gradients. Section 3 presents the derived SGMCMC algorithm for Gaussian process learning. We test our proposed method using a simulation study in Section 4, and present a case study for ocean temperature data in Section 5; Section 6 con-

cludes. A modification of our approach into a stochastic gradient Fisher scoring method for GPs is discussed in the Supplementary Material, alongside its performance for maximum likelihood estimation.

## 2 Matérn Gaussian Process Model and its Approximations

Let  $Y_i$  for  $i \in \{1, \dots, n\}$  be the observation at spatial location  $\mathbf{s}_i = (s_{i1}, s_{i2})$  and  $\mathbf{X}_i = (X_{i1}, \dots, X_{ip})$  be a corresponding vector of covariates. The data-generation model for Gaussian process regression in the case of Gaussian data is

$$Y_i = \mathbf{X}_i \boldsymbol{\beta} + Z(\mathbf{s}_i) + \varepsilon_i, \quad (1)$$

with fixed effects  $\boldsymbol{\beta}$ , spatial process  $Z(\mathbf{s}_i)$  and  $\varepsilon_i \stackrel{iid}{\sim} \text{Normal}(0, \tau^2)$  is measurement error with nugget  $\tau^2$ . The process  $Z(\mathbf{s})$  is an isotropic spatial Gaussian process with mean  $\mathbb{E}\{Z(\mathbf{s})\} = 0$ , spatial variance  $\text{Var}\{Z(\mathbf{s})\} = \sigma^2$  and spatial correlation  $\text{Cor}\{Z(\mathbf{s}_i), Z(\mathbf{s}_j)\} = K(d_{ij})$  for distance  $d_{ij} = \|\mathbf{s}_i - \mathbf{s}_j\|$ . Specifically, we assume the correlation function is the Matérn (Stein, 1999) correlation function with range  $\rho$  and smoothness  $\nu$

$$K(d) = \frac{1}{\Gamma(\nu)2^{\nu-1}} \left(\frac{d}{\rho}\right)^\nu \mathcal{K}_\nu\left(\frac{d}{\rho}\right), \quad (2)$$

where  $\mathcal{K}_\nu$  is the modified Bessel function of the second kind. Let  $\boldsymbol{\theta} = (\sigma^2, \rho, \nu, \tau^2)$  be the collection of covariance parameters.

The marginal distribution (over  $Z$ ) of  $\mathbf{Y} = \{Y(\mathbf{s}_1), \dots, Y(\mathbf{s}_n)\}$  is multivariate normal with mean  $\mathbb{E}[\mathbf{Y}] = \mathbf{X}\boldsymbol{\beta}$ , for  $\mathbf{X} \in \mathbf{R}^{n \times p}$  covariate matrix with the  $i^{\text{th}}$  row  $\mathbf{X}_i$ , and covariance matrix

$\mathbb{E}[(\mathbf{Y} - \mathbf{X}\boldsymbol{\beta})(\mathbf{Y} - \mathbf{X}\boldsymbol{\beta})^T \mid \boldsymbol{\theta}] = \Sigma(\boldsymbol{\theta})$  with

$$\Sigma(\boldsymbol{\theta}) = \sigma^2 \mathbf{K} + \tau^2 \mathbf{I}_n, \quad (3)$$

$$\mathbf{K}_{i,j} = K(d_{ij}).$$

The full log-likelihood then becomes

$$\ell_{\text{full}}(\boldsymbol{\beta}, \boldsymbol{\theta}) = -\frac{n}{2} \log(2\pi) - \frac{1}{2} \log \det \Sigma(\boldsymbol{\theta}) - \frac{1}{2} (\mathbf{Y} - \mathbf{X}\boldsymbol{\beta})^T \Sigma(\boldsymbol{\theta})^{-1} (\mathbf{Y} - \mathbf{X}\boldsymbol{\beta}). \quad (4)$$

Evaluating (4) involves computing the determinant and inverse of  $\Sigma(\boldsymbol{\theta})$  which generally requires  $O(n^3)$  operations. This cost becomes prohibitive for large spatial datasets. The remainder of this section discusses the computationally-efficient Vecchia approximation.

## 2.1 The Vecchia approximation

For any set of spatial locations, the joint distribution of  $\mathbf{Y}$  can be written as a product of univariate conditional distributions, which can then be approximated by a Vecchia approximation (Vecchia, 1988; Stein et al., 2004; Datta et al., 2016; Katzfuss and Guinness, 2021):

$$f(Y(\mathbf{s}_1), \dots, Y(\mathbf{s}_n)) = \prod_{i=1}^n f(Y(\mathbf{s}_i) \mid Y(\mathbf{s}_1), \dots, Y(\mathbf{s}_{i-1})) \approx \prod_{i=1}^n f_i(Y(\mathbf{s}_i) \mid Y(\mathbf{s}_{(i)})), \quad (5)$$

for  $Y(\mathbf{s}_{(i)}) = \{Y(\mathbf{s}_j); j \in \mathcal{N}_i\}$  and conditioning set  $\mathcal{N}_i \subseteq \{1, \dots, i-1\}$ , e.g., the indices of the  $m_i \leq m$  locations in  $\mathcal{N}_i$  that are closest to  $\mathbf{s}_i$  according to some ordering of the data. Here, we use the notation that the collection of variables over the conditioning set of  $Y_i$  is denoted  $Y_{(i)} = \{Y_j; j \in \mathcal{N}_i\}$ . Of course, not all locations that are dependent with location  $i$  need be included in  $\mathcal{N}_i$  because distant observations may be approximately independent after conditioning on more local



observations. Conditioning on only  $\mathcal{N}_i$  leads to substantial computational savings when  $m$  is small, *i.e.*,  $m \ll n$ . The Vecchia approximation is attractive for GPs in particular since the conditional densities are Normally distributed. Stein (2002) proved that a screening effect exists in this context which ensures that the Vecchia approximation is a good approximation, and Stein (2011) provided conditions for a variety of situations when the screening effect might hold. Also, while we have motivated the Vecchia likelihood as an approximation, it is in fact a valid joint probability density function (PDF) which permits a standard Bayesian analysis and interpretation.

Let  $p(\boldsymbol{\beta}, \boldsymbol{\theta})$  be the prior distribution on the regression and covariance parameters. Using (5) we can write the posterior as (ignoring a constant that does not depend on the parameters)

$$\begin{aligned} \ell(\boldsymbol{\beta}, \boldsymbol{\theta}) &= \sum_{i=1}^n \log f(Y(\mathbf{s}_i) \mid Y(\mathbf{s}_{(i)}), \boldsymbol{\beta}, \boldsymbol{\theta}), \\ \log p(\boldsymbol{\beta}, \boldsymbol{\theta} \mid \mathbf{Y}) &= \ell(\boldsymbol{\beta}, \boldsymbol{\theta}) + \log p(\boldsymbol{\beta}, \boldsymbol{\theta}). \end{aligned} \tag{6}$$

Hence the log-likelihood and log-posterior of the parameters  $\{\boldsymbol{\beta}, \boldsymbol{\theta}\}$  can be written as a sum of conditional normal log-densities, where the conditioning set is at most of size  $m$ . The cost of computing the log-posterior in (6) is linear in  $n$  and cubic in  $m$ .

Although the Vecchia approximation reduces the complexity cost from  $O(n^3)$  for the full likelihood to  $O(nm^3)$ , this can still pose challenges for very large  $n$ . We can further reduce the cost of Bayesian inference by using subsampling strategies which have had substantial success in SG methods (Newton et al., 2018). Although we are still in correlated data setting, sampling the summands of (6) with equal probability and without replacement leads to an unbiased estimate of the gradient. Let  $\mathcal{B} \subset \{1, \dots, n\}$  be a subsample, *i.e.*, a minibatch index set of size  $n_{\mathcal{B}}$ , and let

$$\bar{\ell}_{\mathcal{B}}(\boldsymbol{\beta}, \boldsymbol{\theta}) = \frac{n}{n_{\mathcal{B}}} \sum_{i \in \mathcal{B}} \log f(Y(\mathbf{s}_i) \mid Y(\mathbf{s}_{(i)}), \boldsymbol{\beta}, \boldsymbol{\theta}). \tag{7}$$

**Theorem 1.** *The gradient of  $\bar{\ell}_{\mathcal{B}}$  is an unbiased estimator of the gradient of the Vecchia posterior  $\ell(\boldsymbol{\beta}, \boldsymbol{\theta})$ .*

*Proof.*

$$\begin{aligned} \mathbb{E}_{\mathcal{B}}[\nabla \bar{\ell}_{\mathcal{B}}(\boldsymbol{\beta}, \boldsymbol{\theta})] &= \nabla \mathbb{E}_{\mathcal{B}} \left[ \frac{n}{n_{\mathcal{B}}} \sum_{i=1}^n \log f(Y(\mathbf{s}_i) | Y(\mathbf{s}_{(i)}), \boldsymbol{\beta}, \boldsymbol{\theta}) \delta_{i \in \mathcal{B}} \right] \\ &= \nabla \sum_{i=1}^n \log f(Y(\mathbf{s}_i) | Y(\mathbf{s}_{(i)}), \boldsymbol{\beta}, \boldsymbol{\theta}) \\ &= \nabla \ell(\boldsymbol{\beta}, \boldsymbol{\theta}). \end{aligned} \tag{8}$$

□

Using (8), we can construct an unbiased estimate of the gradient of the Vecchia log-posterior based on a minibatch of the data:

$$\bar{g}_{\mathcal{B}}(\boldsymbol{\beta}, \boldsymbol{\theta}) = \nabla \bar{\ell}_{\mathcal{B}}(\boldsymbol{\beta}, \boldsymbol{\theta}) + \nabla \log p(\boldsymbol{\beta}, \boldsymbol{\theta}), \tag{9}$$

hence reducing the cost of learning iterations to be linear in  $n_{\mathcal{B}}$  instead of  $n$ , *i.e.*,  $O(m^3 n_{\mathcal{B}})$ .

### 3 The SG-MCMC Algorithm

In this section we first review the general SG Langevin dynamics method and then present the proposed algorithm based on the Vecchia approximation.

#### 3.1 SG Langevin Dynamics

SG Markov chain Monte Carlo (Ma et al., 2015) is a popular method for scalable Bayesian inference. SGMCMC proceeds by simulating continuous dynamics of a potential energy, namely

the negative log-posterior  $-\log p(\boldsymbol{\beta}, \boldsymbol{\theta} \mid \mathbf{Y})$ , such that the dynamics generate samples from the posterior distribution. Let  $\boldsymbol{\phi} = (\boldsymbol{\beta}^\top, \boldsymbol{\theta}^\top)^\top$  be the parameter vector concatenating the regression and covariance parameters of the Gaussian process regression model. The Langevin diffusion over  $\log p(\boldsymbol{\phi} \mid \mathbf{Y})$  is given by the stochastic differential equation (SDE)

$$d(\boldsymbol{\phi}_t) = \nabla \log p(\boldsymbol{\phi}_t \mid \mathbf{Y})dt + \sqrt{2}dW_t, \quad (10)$$

where  $dW_t$  is Brownian motion and the index  $t$  represents time. The distribution of samples  $\boldsymbol{\phi}_t$  converges to the true posterior as  $t \rightarrow \infty$  (Roberts and Rosenthal, 1998).

Since simulating a continuous time process is infeasible, in practice a discretized numerical approximation is used. Here we use the Euler discretization method. Let  $h_t$  the step size at time  $t$ , and let  $\boldsymbol{\phi}_t$  the current value of the parameter. The Euler approximation of the Langevin dynamics is given by

$$\boldsymbol{\phi}_{t+1} = \boldsymbol{\phi}_t + h_t \nabla \log p(\boldsymbol{\phi}_t \mid \mathbf{Y}) + \sqrt{2h_t}e_t, \quad (11)$$

where  $e_t$  is random white noise. This recursive sampling approach is known as the Langevin Monte Carlo algorithm. Often, a Metropolis-Hastings (MH) correction step is added to account for the discretization error.

When the size of the dataset is large, computing the log-posterior gradient represents a computational bottleneck. To overcome this problem, the key idea of SGLD is to replace  $\nabla \log p(\boldsymbol{\phi} \mid \mathbf{Y})$  with an unbiased gradient estimate, *i.e.*,  $\bar{g}_B(\boldsymbol{\phi})$  in (9) that is computationally cheaper to compute, and use a decreasing step size  $h_t$  to avoid the costly M-H correction steps,

$$\text{SGLD : } \quad \boldsymbol{\phi}_{t+1} = \boldsymbol{\phi}_t + h_t \bar{g}_B(\boldsymbol{\phi}_t) + \sqrt{2h_t}e_t. \quad (12)$$

In order to assure convergence to the true posterior the step sizes must satisfy

$$0 < h_{t+1} < h_t, \sum_{t=1}^{\infty} h_t = \infty, \text{ and } \sum_{t=1}^{\infty} h_t^2 < \infty.$$

The SGLD step in (12) updates all parameters using the same step size. This can cause slow mixing when different parameters have different curvature or scales. SG Riemannian Langevin Dynamics (SGRLD) takes account of the difference in curvature and scale by using an appropriate Riemannian metric  $G(\phi)$ , and simulates the diffusion by preconditioning the unbiased gradient and noise in (12) using  $G^{-1}(\phi)$ . SGRLD achieves better mixing by incorporating geometric information of the posterior. Commonly used metrics for  $G(\phi)$  include the Fisher information matrix and estimates of the Hessian of the log-posterior. Given a preconditioning matrix  $G(\phi)$ , the SGRLD step is

$$\text{SGRLD} \quad \phi_{t+1} = \phi_t + h_t (G^{-1}(\phi_t) \bar{g}_{\mathcal{B}}(\phi_t) + \Gamma(\phi_t)) + \sqrt{2h_t} G^{-1/2}(\phi_t) e_t, \quad (13)$$

where the term  $\Gamma(\phi_t)$  represents the drift term that describes how the preconditioner  $G(\phi_t)$  changes with respect to  $\phi_t$ . The drift term is given by

$$\Gamma(\phi_t)_i = \sum_j \frac{\partial G(\phi_t)_{ij}^{-1}}{\partial \phi_{tj}}. \quad (14)$$

The drift term vanishes in the SGLD step since the preconditioner is assumed to be the identity matrix. The SGRLD algorithm in (13) takes steps in the steepest ascent on the manifold defined by the metric  $G(\phi_t)$ . For many statistical models, the Fisher information matrix is intractable, however we will show in the next section that using the Vecchia's approximation we can compute the Fisher information and its inverse without incurring a high computational cost. Therefore, we use the Fisher information matrix, denoted  $\mathcal{I}(\phi)$ , for  $G(\phi)$ .

### 3.2 Derivation of gradients and Fisher information for SGRLD

Given an index set for a mini-batch subset of the data  $\mathcal{B}$ , the log-likelihood in (7) decomposes as the sum of log-conditional densities of the  $Y(\mathbf{s}_i)$  given the conditioning points  $Y(\mathbf{s}_{(i)})$ . Computing the gradient of these conditional densities is analytically complicated and not computationally tractable. We follow Guinness (2019) to first rewrite the log-conditional densities in terms of marginal densities, and then compute the gradients and Fisher information. Let  $u_i = Y(\mathbf{s}_{(i)})$ , the set of neighbours, and  $v_i = (Y(\mathbf{s}_{(i)}), Y(\mathbf{s}_i))$ , the vector of concatenating the  $i^{\text{th}}$  observation and its neighbours. Let  $\mathbf{Q}_i$  and  $\mathbf{R}_i$  be the covariate matrices for  $u_i$  and  $v_i$  respectively, and let  $\mathbf{A}_i$  and  $\mathbf{B}_i$  denote the covariance matrices of  $u_i$  and  $v_i$ . The minibatch log-likelihood in (7) can thus be written as

$$\begin{aligned} \bar{\ell}_{\mathcal{B}}(\boldsymbol{\phi}) &= \sum_{i \in \mathcal{B}} \log f(v_i | \boldsymbol{\phi}) - \log f(u_i | \boldsymbol{\phi}) \\ &= -\frac{1}{2} \sum_{i \in \mathcal{B}} \log \det \mathbf{B}_i - \log \det \mathbf{A}_i \\ &\quad - \frac{1}{2} \sum_{i \in \mathcal{B}} [(v_i - \mathbf{R}_i \boldsymbol{\beta})^{\text{T}} \mathbf{B}_i^{-1} (v_i - \mathbf{R}_i \boldsymbol{\beta}) - (u_i - \mathbf{Q}_i \boldsymbol{\beta})^{\text{T}} \mathbf{A}_i^{-1} (u_i - \mathbf{Q}_i \boldsymbol{\beta})] - \frac{n_{\mathcal{B}}}{2} \log(2\pi). \end{aligned} \quad (15)$$

In order to compute the log-likelihood, we need the following quantities

$$p_{\mathcal{B}}^1(\boldsymbol{\theta}) = \sum_{i \in \mathcal{B}} \log \det \mathbf{B}_i - \log \det \mathbf{A}_i \quad (16)$$

$$p_{\mathcal{B}}^2(\boldsymbol{\theta}) = \sum_{i \in \mathcal{B}} (v_i^{\text{T}} \mathbf{B}_i^{-1} v_i - u_i^{\text{T}} \mathbf{A}_i^{-1} u_i) \quad (17)$$

$$p_{\mathcal{B}}^3(\boldsymbol{\theta}) = \sum_{i \in \mathcal{B}} (\mathbf{R}_i^{\text{T}} \mathbf{B}_i^{-1} v_i - \mathbf{Q}_i^{\text{T}} \mathbf{A}_i^{-1} u_i) \quad (18)$$

$$p_{\mathcal{B}}^4(\boldsymbol{\theta}) = \sum_{i \in \mathcal{B}} (\mathbf{R}_i^{\text{T}} \mathbf{B}_i^{-1} \mathbf{R}_i - \mathbf{Q}_i^{\text{T}} \mathbf{A}_i^{-1} \mathbf{Q}_i). \quad (19)$$

The quantities in (16) - (19) only depend on the covariance parameters  $\boldsymbol{\theta}$  via  $\mathbf{A}_i$  and  $\mathbf{B}_i$  and not the mean parameters  $\boldsymbol{\beta}$ . We can now write the minibatch log-likelihood as

$$\bar{\ell}_{\mathcal{B}}(\boldsymbol{\phi}) = -\frac{n_{\mathcal{B}}}{2} \log(2\pi) - \frac{1}{2} [p_{\mathcal{B}}^1(\boldsymbol{\theta}) + p_{\mathcal{B}}^2(\boldsymbol{\theta}) - 2\boldsymbol{\beta}^T p_{\mathcal{B}}^3(\boldsymbol{\theta}) + \boldsymbol{\beta}^T p_{\mathcal{B}}^4(\boldsymbol{\theta}) \boldsymbol{\beta}]. \quad (20)$$

### 3.2.1 Mean parameters

The gradient of the minibatch log-likelihood with respect to the mean parameters  $\boldsymbol{\beta}$  is

$$\frac{\partial \bar{\ell}_{\mathcal{B}}(\boldsymbol{\beta}, \boldsymbol{\theta})}{\partial \boldsymbol{\beta}} = p_{\mathcal{B}}^3(\boldsymbol{\theta}) - p_{\mathcal{B}}^4(\boldsymbol{\theta}) \boldsymbol{\beta}. \quad (21)$$

For the Fisher information, recall that if a random vector follows a multivariate normal model with mean and variance parameterized by two different parameter vectors, *i.e.*,  $W \sim \mathbf{N}(\mu(\boldsymbol{\beta}), \Sigma(\boldsymbol{\theta}))$ , then the Fisher information is block diagonal  $\mathcal{I}(\boldsymbol{\phi}) = \text{diag}(\mathcal{I}(\boldsymbol{\beta}), \mathcal{I}(\boldsymbol{\theta}))$ . Furthermore, let  $J_{\boldsymbol{\beta}}$  be the Jacobian of  $\mu(\boldsymbol{\beta})$  with respect to  $\boldsymbol{\beta}$ . Then the Fisher information matrix is analytically available (Mardia and Marshall, 1984) and takes the form

$$\mathcal{I}(\boldsymbol{\beta}) = J_{\boldsymbol{\beta}} \Sigma^{-1} J_{\boldsymbol{\beta}}^T \quad (22)$$

$$\mathcal{I}(\boldsymbol{\theta})_{jk} = \frac{1}{2} \text{Tr} \left( \Sigma^{-1} \frac{\partial \Sigma}{\partial \boldsymbol{\theta}_j} \Sigma^{-1} \frac{\partial \Sigma}{\partial \boldsymbol{\theta}_k} \right). \quad (23)$$

Using (22) and the chain rule property of the Fisher information,  $\mathcal{I}_{Y(s_i)|u_i}(\boldsymbol{\phi}) = \mathcal{I}_{v_i}(\boldsymbol{\phi}) - \mathcal{I}_{u_i}(\boldsymbol{\phi})$  and summing over the components of the log-likelihood we get

$$\mathcal{I}_{\mathcal{B}}(\boldsymbol{\beta}) = \sum_{i \in \mathcal{B}} (\mathbf{R}_i^T \mathbf{B}_i^{-1} \mathbf{R}_i - \mathbf{Q}_i^T \mathbf{A}_i^{-1} \mathbf{Q}_i) = p_{\mathcal{B}}^4(\boldsymbol{\theta}). \quad (24)$$

Hence the Fisher information of  $\boldsymbol{\beta}$  is constant with respect to the mean parameters. In addition,

since  $\mathcal{I}(\phi)$  is block diagonal, the drift term which represents how  $\mathcal{I}(\beta)$  changes with respect to  $\phi$  is  $\Gamma_{\mathcal{B}}(\beta) = \mathbf{0}_p$ . The SGRLD step for regression parameters is thus

$$\beta_{t+1} = \beta_t + h_t p_{\mathcal{B}}^4(\theta_t)^{-1} (p_{\mathcal{B}}^3(\theta_t) - p_{\mathcal{B}}^4(\theta_t)\beta_t) + \sqrt{2h_t} p_{\mathcal{B}}^4(\theta)^{-1/2} e_t. \quad (25)$$

### 3.2.2 Covariance parameters

For the covariance parameters, we first start by computing the partial derivatives of the quantities defined in (16)-(19) with respect to the components of  $\theta$ ,  $p_j^k(\theta) = \partial p_{\mathcal{B}}^k(\theta) / \partial \theta_j$  for  $j \in \{1, \dots, 4\}$

$$p_j^1(\theta) = \sum_{i \in \mathcal{B}} \left( \text{Tr}(\mathbf{B}_i^{-1} \frac{\partial \mathbf{B}_i}{\partial \theta_j}) - \text{Tr}(\mathbf{A}_i^{-1} \frac{\partial \mathbf{A}_i}{\partial \theta_j}) \right) \quad (26)$$

$$p_j^2(\theta) = \sum_{i \in \mathcal{B}} \left( v_i^{\text{T}} \mathbf{B}_i^{-1} \frac{\partial \mathbf{B}_i}{\partial \theta_j} \mathbf{B}_i^{-1} v_i - u_i^{\text{T}} \mathbf{A}_i^{-1} \frac{\partial \mathbf{A}_i}{\partial \theta_j} \mathbf{A}_i^{-1} u_i \right) \quad (27)$$

$$p_j^3(\theta) = \sum_{i \in \mathcal{B}} \left( \mathbf{R}_i^{\text{T}} \mathbf{B}_i^{-1} \frac{\partial \mathbf{B}_i}{\partial \theta_j} \mathbf{B}_i^{-1} v_i - \mathbf{Q}_i^{\text{T}} \mathbf{A}_i^{-1} \frac{\partial \mathbf{A}_i}{\partial \theta_j} \mathbf{A}_i^{-1} u_i \right) \quad (28)$$

$$p_j^4(\theta) = \sum_{i \in \mathcal{B}} \left( \mathbf{R}_i^{\text{T}} \mathbf{B}_i^{-1} \frac{\partial \mathbf{B}_i}{\partial \theta_j} \mathbf{B}_i^{-1} \mathbf{R}_i - \mathbf{Q}_i^{\text{T}} \mathbf{A}_i^{-1} \frac{\partial \mathbf{A}_i}{\partial \theta_j} \mathbf{A}_i^{-1} \mathbf{Q}_i \right) \quad (29)$$

$$\frac{\partial \bar{\ell}_{\mathcal{B}}(\beta, \theta)}{\partial \theta_j} = -\frac{1}{2} [p_j^1(\theta) + p_j^2(\theta) - 2p_j^3(\theta)\beta + \beta^{\text{T}} p_j^4(\theta)\beta]. \quad (30)$$

Using (23) and the chain rule decomposition of the Fisher information, we derive the analytic form of the Fisher information and drift term for the covariance parameters

$$\mathcal{I}_{\mathcal{B}}(\theta)_{jk} = \frac{1}{2} \sum_{i \in \mathcal{B}} \text{Tr} \left( \mathbf{B}_i^{-1} \frac{\partial \mathbf{B}_i}{\partial \theta_j} \mathbf{B}_i^{-1} \frac{\partial \mathbf{B}_i}{\partial \theta_k} \right) - \text{Tr} \left( \mathbf{A}_i^{-1} \frac{\partial \mathbf{A}_i}{\partial \theta_j} \mathbf{A}_i^{-1} \frac{\partial \mathbf{A}_i}{\partial \theta_k} \right) \quad (31)$$

$$\begin{aligned} \frac{\partial \mathcal{I}_{\mathcal{B}}(\theta)_{jk}}{\partial \theta_k} &= \sum_{i \in \mathcal{B}} \text{Tr} \left( \mathbf{B}_i^{-1} \frac{\partial^2 \mathbf{B}_i}{\partial \theta_j \partial \theta_k} \mathbf{B}_i^{-1} \frac{\partial \mathbf{B}_i}{\partial \theta_k} \right) - \text{Tr} \left( \mathbf{B}_i^{-1} \frac{\partial \mathbf{B}_i}{\partial \theta_j} \mathbf{B}_i^{-1} \frac{\partial \mathbf{B}_i}{\partial \theta_k} \mathbf{B}_i^{-1} \frac{\partial \mathbf{B}_i}{\partial \theta_k} \right) \\ &\quad - \sum_{i \in \mathcal{B}} \text{Tr} \left( \mathbf{A}_i^{-1} \frac{\partial^2 \mathbf{A}_i}{\partial \theta_j \partial \theta_k} \mathbf{A}_i^{-1} \frac{\partial \mathbf{A}_i}{\partial \theta_k} \right) - \text{Tr} \left( \mathbf{A}_i^{-1} \frac{\partial \mathbf{A}_i}{\partial \theta_j} \mathbf{A}_i^{-1} \frac{\partial \mathbf{A}_i}{\partial \theta_k} \mathbf{A}_i^{-1} \frac{\partial \mathbf{A}_i}{\partial \theta_k} \right) \end{aligned} \quad (32)$$

$$\Gamma_{\mathcal{B}}(\boldsymbol{\theta})_j = - \sum_k \mathcal{I}_{\mathcal{B}}(\boldsymbol{\theta})_j^{-1} \frac{\partial \mathcal{I}_{\mathcal{B}}(\boldsymbol{\theta})}{\partial \theta_k} \mathcal{I}_{\mathcal{B}}(\boldsymbol{\theta})_k^{-1}. \quad (33)$$

## 4 Simulation Study

In this section, we test our proposed SGRLD method in (13) method on synthetic data and assess its performance against state-of-the-art Bayesian methods. We use Mean Squared Error (MSE) and coverage of credible intervals of posterior MCMC estimators to evaluate estimation of the spatial covariance parameters, and we use the Effective sample sizes (ESS) (Heidelberger and Welch, 1981) per minute to gauge computational efficiency of MCMC algorithms. We present results only for the spatial covariance parameters  $\boldsymbol{\theta}$  because the results are similar across methods for  $\boldsymbol{\beta}$ .

### 4.1 Data generation

We generate data on a regular rectangular grid formed with  $n_1$  locations on the x-axis and  $n_2$  on the y-axis, with a total number of points  $N = n_1 n_2$  and grid spacing one. We consider  $N = \{10^4, 10^5, 10^6\}$  for  $n_1 = \{100, 300, 1000\}$  and  $n_2 = N/n_1$ . We generate the Gaussian process  $Z(\mathbf{s})$  from a Matérn kernel with possible smoothness values  $\nu \in \{0.5, 1.0, 1.5\}$ . The range parameter  $\rho$  is chosen such that the correlation function is approximately  $10^{-4}$  for the maximum distance between two points in the grid. We fix the spatial variance  $\sigma^2 = 5$ , and consider different scenarios for the observation noise based on the proportion of variance  $\kappa = \tau^2/\sigma^2 \in \{0.2, 1.0, 5.0\}$ . Let  $\mathbf{X}_i = (1, x_i)$ , the covariate for the  $i^{\text{th}}$  site, the mean of the Gaussian process will take the form  $\mathbb{E}[Y(\mathbf{s}_i)] = \beta_0 + \beta_1 \cos(x_i)$ , where  $\beta_0 = -3$ , and  $\beta_1 = 5$ , and  $x_i \stackrel{iid}{\sim} \text{Uniform}(-3, 3)$ . For  $N = 10^6$ , generating a Gaussian process is computationally infeasible, thus we generate a Vecchia approximated Gaussian process with  $m = 120$  neighbors for each site. For each  $N$ , we generate 100 datasets and record the posterior mean and posterior credible intervals for each parameter.



## 4.2 Competing methods and metrics

We compare our SGRLD method with four different MCMC methods. The first three are SG methods with adaptive drifts. The last method uses the full dataset to sample the posterior distribution using the Vecchia approximation. The three SGMCMC methods all use momentum and past gradient information to estimate the curvature and accelerate the convergence. These methods extend the momentum methods used in SG optimization methods for faster exploration of the posterior. The first method is Preconditioned SGLD (pSGLD) of Li et al. (2016a) that uses the Root Mean Square Propagation (RMSPROP) (Hinton et al., 2012) algorithm to estimate a diagonal preconditioner for the minibatch gradient and injected noise. The second method is ADAMSGLD (Kim et al., 2022) that extends the widely used ADAM optimizer (Kingma and Ba, 2014) to the SGLD setting. ADAMSGLD approximates the first-order and second-order moments of the minibatch gradients to construct a preconditioner. Finally, we also include the performance of Momentum SGLD (MSGLD) where no preconditioner is used but past gradient information is used to accelerate the exploration of the posterior. The details of the above algorithms are included in the Appendix A.1. The final method we consider is the Nearest Neighbor Gaussian Process (NNGP) method (Datta et al., 2016). This method is the standard MCMC method based on the Vecchia approximation and is implemented in the R package spNNGP (Finley et al., 2022). For this method, the initial values are set to the true values and the Metropolis-Hastings proposal distribution is chosen adaptively using the default settings.

For the SGMCMC methods, the batch size is set to 250 when the number of location is  $10^4$  and 500 for the other two cases. We noticed during our experiments that batch sizes in the order of 200 perform better than smaller size ones, with very similar performance to larger ones. The number of epochs will depend on the size of data, and is chosen such that the total number of iterations is 20000, of which a quarter are discarded as burn-in. The learning rate is divided by a factor of 2

every 5 epochs, so the final learning rate is set at 1% of the initial value. A first tentative value of the learning rate is set at  $1/N$ , then reduced until the norm of the first step is less than one. We noticed that the appropriate learning rate for our SGRLD method is within one to two orders of magnitude large than the learning rate for the other SG sampling methods. For all the methods, the size of the conditioning set is fixed at  $m = 15$ . The conditioning sets were selected using the max-min ordering (Katzfuss and Guinness, 2021) for  $N < 10^6$ , and random ordering otherwise. Katzfuss and Guinness (2021) showed that the max-min ordering results in significant improvements over other coordinate based orderings. However, when  $N$  is very large, the cost of max-min ordering becomes prohibitive. For the NNGP method, we take 2000 samples when  $N < 10^5$  and 1000 otherwise. For all the methods we use a non-informative flat prior on the regression parameters. For the covariance parameters, we set the following priors:

$$\rho \sim \text{Gamma}(9.0, 2.0)$$

$$\nu \sim \text{Log-Normal}(1.0, 1.0)$$

$$\tau^2, \sigma^2 \sim \text{Gamma}(0.1, 0.1)$$

The prior 90% credible intervals for  $\rho$  and  $\nu$  are (2.06, 7.88) and (0.52, 14.08) respectively, which represent weakly informative priors.

### 4.3 Results

Table 1 gives the MSE results. Our SGRLD method outperforms all the others with very low MSE across parameters. In particular, the SGMCMC methods all outperform the NNGP method. In our experiments, we noticed that the NNGP method suffers from very slow mixing due to the M-H step necessary for sampling the covariance parameters. In fact, even if we start the

Table 1: Mean squared error (Monte Carlo standard errors) of covariance parameters computed using 100 simulations, each having sample size  $N$ . The proposed SGRLD method compared with other SGMCMC methods (pSGLD, ADAMSGLD, MSGLD) and the full likelihood NNGP method.

N	Algorithm	Variance ( $\sigma^2$ )	Range ( $\rho$ )	Smoothness ( $\nu$ )	Nugget ( $\tau^2$ )
$10^4$	pSGLD	0.074(0.013)	0.039(0.008)	0.103(0.017)	0.002( $4 \cdot 10^{-4}$ )
	ADAMSGLD	0.075(0.017)	0.036(0.008)	0.129(0.023)	0.002( $6 \cdot 10^{-4}$ )
	MSGLD	0.066(0.014)	0.034(0.008)	0.108(0.0196)	0.002( $6 \cdot 10^{-4}$ )
	NNGP	0.414(0.131)	0.095(0.071)	0.162(0.106)	0.093( $2.4 \cdot 10^{-2}$ )
	SGRLD	0.056(0.016)	0.031(0.006)	0.077(0.013)	0.001( $10^{-4}$ )
$10^5$	pSGLD	0.008(0.001)	0.002(0.0003)	0.011(0.0019)	$1 \cdot 10^{-4}$ ( $2 \cdot 10^{-5}$ )
	ADAMSGLD	0.014(0.005)	0.008(0.002)	0.031(0.008)	$1 \cdot 10^{-4}$ ( $2 \cdot 10^{-4}$ )
	MSGLD	0.017(0.001)	0.003( $5 \cdot 10^{-4}$ )	0.019(0.002)	$2 \cdot 10^{-4}$ ( $4 \cdot 10^{-5}$ )
	NNGP	0.116(0.030)	0.024(0.01)	0.118(0.08)	$4 \cdot 10^{-2}$ (0.01)
	SGRLD	0.005( $8 \cdot 10^{-4}$ )	0.001( $1.0 \cdot 10^{-4}$ )	0.008( $1.8 \cdot 10^{-3}$ )	$10^{-4}$ ( $2 \cdot 10^{-5}$ )
$10^6$	pSGLD	0.003(0.001)	0.003(0.0008)	0.002(0.0014)	$3.1 \cdot 10^{-4}$ ( $6 \cdot 10^{-5}$ )
	ADAMSGLD	0.009(0.002)	0.006(0.002)	0.026(0.007)	$2 \cdot 10^{-4}$ ( $9 \cdot 10^{-5}$ )
	MSGLD	0.011( $1.8 \cdot 10^{-3}$ )	0.003( $5 \cdot 10^{-4}$ )	0.019(0.002)	$1 \cdot 10^{-5}$ ( $3 \cdot 10^{-5}$ )
	NNGP	0.078(0.055)	0.016(0.009)	0.126(0.086)	0.08(0.049)
	SGRLD	0.002( $3 \cdot 10^{-4}$ )	0.001( $1 \cdot 10^{-4}$ )	0.004( $6.1 \cdot 10^{-3}$ )	$0.4 \cdot 10^{-4}$ ( $1 \cdot 10^{-5}$ )

NNGP sampling process at true values of the covariance parameters, and reduce the variance of the proposal distribution, the acceptance rate of the M-H step stays below 15%. None of the SGMCMC methods requires any such step as long as the learning rate is kept small.

Table 2 summarizes the results for the coverage of the 95% credible intervals. Our SGRLD method again outperforms the other methods. One exception is that the pSGLD algorithm surpasses the SGRLD in the coverage of the variance parameter. Across methods, the smoothness parameter consistently has the lowest coverage, followed by the range parameter. Even for  $N = 10^6$ , MSGLD, ADAMSGLD and NNGP fail to attain a 90% coverage rate. Whilst the SGRLD coverage rate for both parameters is higher than 90% even for  $N = 10^4$ .

For the ESS results in Table 3, the SGRLD method offers superior effective samples per unit time for all the parameters. The pSGLD and MSGLD method seem to adapt to the curvature of the variance parameter, with pSGLD offering higher effective samples than SGRLD. This suggests that the computed preconditioner in pSGLD adapts mainly to the curvature of the variance term,

Table 2: Coverage of the 95% credible intervals (Monte Carlo standard errors) for the covariance parameters computed using 100 simulations, each having sample size  $N$ . The proposed SGRLD method is compared with other SGMCMC methods (pSGLD, ADAMSGLD, MSGLD) and the full likelihood NNGP method.

N	Algorithm	Variance, $\sigma^2$	Range, $\rho$	Smoothness, $\nu$	Nugget, $\tau^2$
$10^4$	pSGLD	0.977(0.02)	0.845(0.06)	0.815(0.06)	0.931(0.05)
	ADAMSGLD	0.886(0.05)	0.791(0.08)	0.647(0.08)	0.636(0.05)
	MSGLD	0.793(0.03)	0.847(0.07)	0.709(0.07)	0.683(0.05)
	NNGP	0.783(0.06)	0.776(0.05)	0.614(0.07)	0.812(0.01)
	SGRLD	0.955(0.03)	0.924(0.05)	0.909(0.04)	0.935(0.01)
$10^5$	pSGLD	0.991(0.03)	0.913(0.04)	0.862(0.05)	0.965(0.02)
	ADAMSGLD	0.861(0.03)	0.754(0.07)	0.814(0.03)	0.738(0.05)
	MSGLD	0.896(0.04)	0.881(0.07)	0.774(0.08)	0.872(0.07)
	NNGP	0.826(0.05)	0.758(0.04)	0.714(0.03)	0.872(0.02)
	SGRLD	0.957(0.01)	0.964(0.01)	0.948(0.01)	0.932( $5 \cdot 10^{-3}$ )
$10^6$	pSGLD	0.987( $6 \cdot 10^{-3}$ )	0.934(0.02)	0.901(0.03)	0.961(0.01)
	ADAMSGLD	0.902(0.01)	0.824( $10^{-3}$ )	0.838(0.02)	0.781(0.03)
	MSGLD	0.884( $10^{-3}$ )	0.918(0.02)	0.846(0.01)	0.926(0.01)
	NNGP	0.866(0.03)	0.818(0.06)	0.834(0.04)	0.862(0.01)
	SGRLD	0.968( $6 \cdot 10^{-3}$ )	0.941( $8 \cdot 10^{-3}$ )	0.929( $5 \cdot 10^{-3}$ )	0.941( $2 \cdot 10^{-3}$ )

but fails to measure the curvature of the smoothness and range. A similar behavior is also observed in the other two methods, MSGLD and ADAMSGLD. On the other hand, the ESS for SGRLD is of the same order for all the parameters. We believe this indicates that using the Fisher information matrix as a Riemannian metric provides an accurate measure of the curvature and results in higher effective samples for all the parameters. The NNGP method provides low effective sample sizes compared to the other three methods due to the low acceptance rate from the MH correction step.

Given the performance of the SG based methods in this simulation study, especially the SGRLD, we conducted an additional simulation study where we focus on point estimates instead of fully Bayesian inference. In Appendix A.2, we tweak the SGRLD method and turn it into a SG Fisher scoring (SGFS) algorithm for point estimates. We compare this method to the full data gradient Fisher scoring method (Guinness, 2019) already implemented in the GpGp R package (Guinness et al., 2018). We find improved speed and estimation precision compared to the GpGp package.

Table 3: Effective sample size per minute (Monte Carlo standard errors) of covariance parameters computed using 100 simulations, each having sample size  $N$ . The proposed SGRLD method is compared with other SGMCMC methods (pSGLD, ADAMSGLD, MSGLD) and the full likelihood NNGP method.

N	Algorithm	Variance, $\sigma^2$	Range, $\rho$	Smoothness, $\nu$	Nugget, $\tau^2$
$10^4$	pSGLD	42.97(1.57)	8.43(0.54)	4.33(0.26)	9.82(0.79)
	ADAMSGLD	9.12(0.45)	4.22(0.33)	2.85(0.28)	3.80(0.48)
	MSGLD	15.68(0.95)	6.48(0.70)	3.65(0.44)	5.11(0.78)
	NNGP	1.02(0.33)	0.99(0.24)	1.11(0.75)	0.51(0.14)
	SGRLD	23.8(1.15)	23.9(1.19)	25.2(1.25)	30.5(1.55)
$10^5$	pSGLD	66.87(2.09)	10.06(0.65)	3.59(0.21)	11.3(0.79)
	ADAMSGLD	7.87(0.38)	2.37(0.27)	1.15(0.13)	1.64(0.24)
	MSGLD	12.92(0.67)	3.15(0.36)	1.206(0.11)	1.71(0.13)
	NNGP	0.89(0.08)	0.75(0.31)	1.02(0.14)	0.47(0.07)
	SGRLD	22.7(0.33)	22.44(0.27)	22.69(0.13)	23.23(0.34)
$10^6$	pSGLD	96.49(3.37)	13.68(0.81)	3.04(0.11)	9.74(0.42)
	ADAMSGLD	6.17(0.13)	4.56(0.52)	1.98(0.62)	2.36(0.83)
	MSGLD	15.07(1.01)	3.78(0.81)	2.06(0.30)	5.01(0.97)
	NNGP	0.81(0.16)	1.01(0.34)	0.28(0.05)	0.52(0.03)
	SGRLD	25.8(0.14)	26.05(0.18)	29.62(0.28)	24.07(0.27)

## 5 Analysis of Global Ocean Temperature Data

We apply the proposed method to the ocean temperature data provided by the Argo Program (Argo, 2023) made available through the `GpGp` package (Guinness et al., 2018). Each of the  $n = 32,436$  observations are taken on buoys in the Spring of 2016. Each observation measures of ocean temperature (C) at depths of roughly 100, 150 and 200 meters. The data are plotted in Figure 1 for depth 100 meters; we analyze these data using the methods evaluated in Section 4. As an illustrative example, the mean function is taken to be quadratic in latitude and longitude and the covariance function is the isotropic Matérn covariance function used in Section 4. All prior distributions and MCMC settings are the same as in Section 4.

We first split the data into a test and training set, keeping 20% of the observations in the testing set. We train the models using 8000 and 40000 MCMC iterations for the NNGP and SGRLD method respectively. For the SGRLD method this requires only 400 epochs. We compare our SGRLD with the NNGP method using prediction MSE, squared correlation between predicted and observed ( $R^2$ )

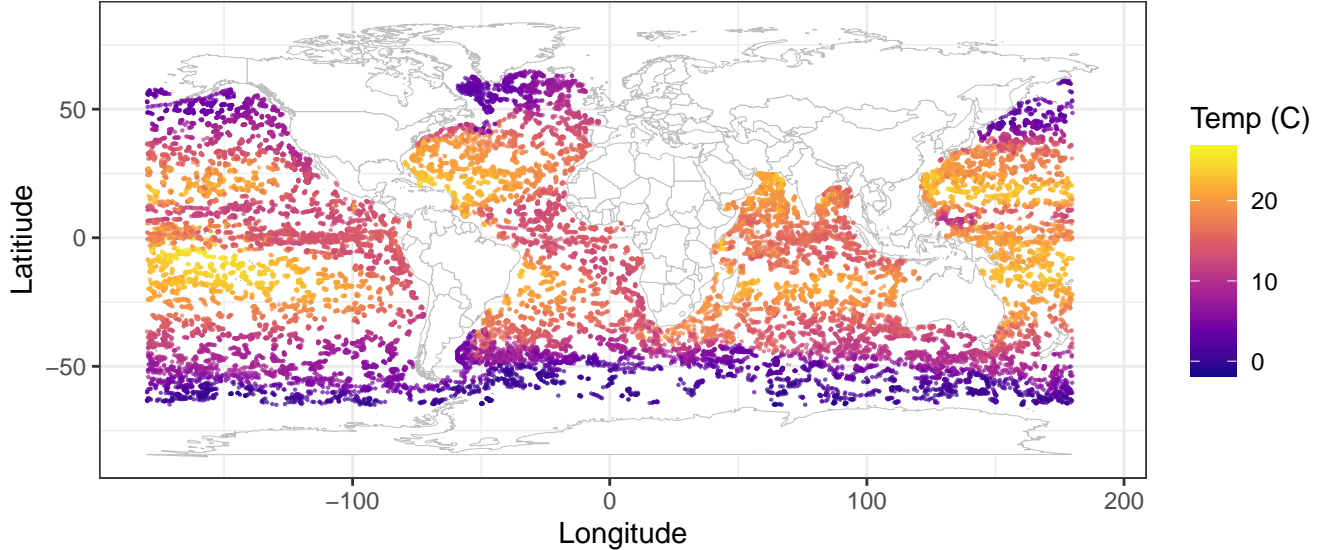


Figure 1: Argo ocean temperature measurements at a depth of 100 meters.

	MSE	Coverage	$R^2$	Time (in minutes)
NNGP	6.41	0.88	0.89	218.55
SGRLD	1.47	0.93	0.94	7.01

Table 4: Prediction Mean Squared Error (MSE), squared correlation between predicted and observed ( $R^2$ ) and coverage rate of the 95% predictive credible intervals on the test set and the correlation between the predicted temperatures and true observed values. The last column gives the total training time in minutes. We take 8000 and 40000 samples using the NNGP and SGRLD method respectively.

and coverage of 95% prediction intervals on the test set. We also include the effective sample size per minute for all the model parameters.

Table 4 gives the MSE and coverage rate on the testing set, and total training time respectively. Our method achieves less than the quarter of the MSE of NNGP while also requiring less than a twentieth of the time. For the coverage of the 95% prediction intervals, the NNGP method’s average coverage on the testing set is significantly lower than the nominal value, while our proposed method achieves 93% coverage.

Table 5 gives the posterior mean, 95% interval and effective sample size per minute for the

Method	Parameter	Posterior mean	95% CI	ESS/min
NNGP	$\sigma^2$	6.72	(6.32, 7.08)	0.17
	$\rho$	0.10	(0.10, 0.11)	3.42
	$\nu$	0.33	(0.32, 0.34)	0.04
	$\tau^2$	0.08	(0.08, 0.09)	0.08
SGRLD	$\sigma^2$	10.64	(7.41, 13.57)	52.21
	$\rho$	48.93	(22.94, 68.46)	115.41
	$\nu$	0.25	(0.23, 0.27)	18.68
	$\tau^2$	0.04	(0.03, 0.05)	39.13

Table 5: Posterior mean, 95% credible intervals and effective sample size per minute for all the covariance parameters.

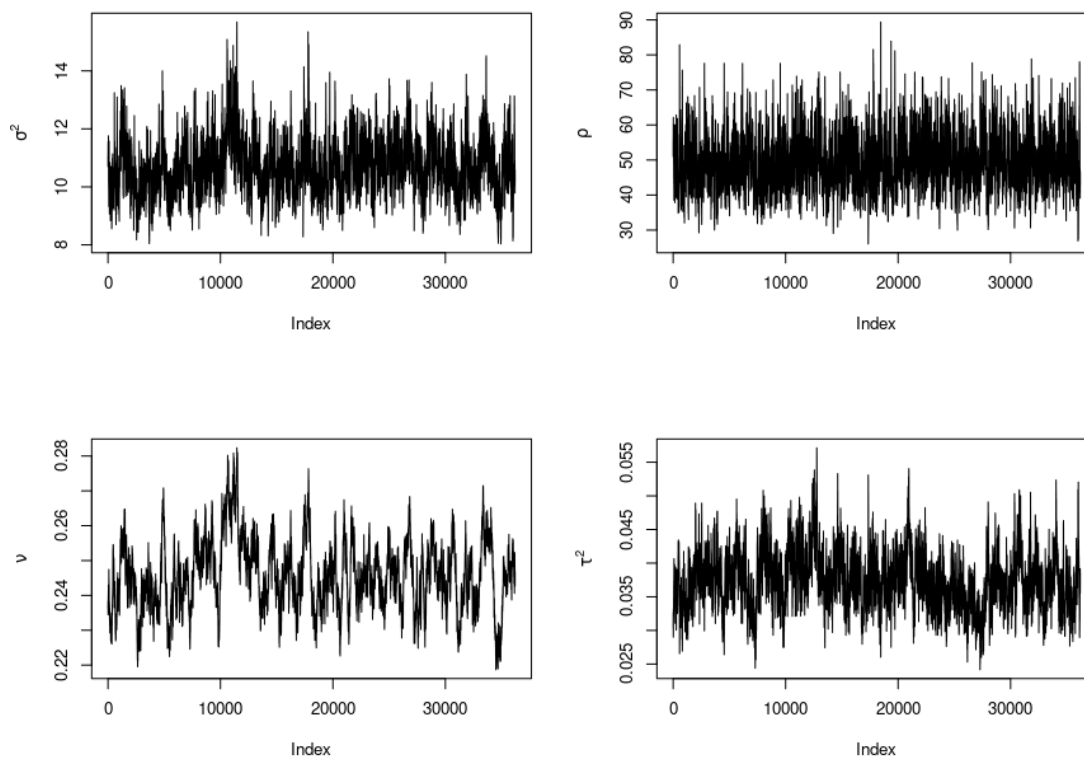


Figure 2: Evolution of SGRLD sampling from the posterior distribution of the covariance parameters.

$n_B$	$m$	$\sigma^2$	$\rho$	$\nu$	$\tau^2$
100	10	10.18 <sub>(8.79,11.89)</sub>	53.67 <sub>(41.11,66.87)</sub>	0.24 <sub>(0.22,0.25)</sub>	0.04 <sub>(0.03,0.04)</sub>
	15	11.29 <sub>(9.08,13.53)</sub>	54.95 <sub>(39.18,72.83)</sub>	0.25 <sub>(0.22,0.27)</sub>	0.04 <sub>(0.03,0.04)</sub>
	30	9.60 <sub>(5.09,13.24)</sub>	46.41 <sub>(13.34,74.52)</sub>	0.24 <sub>(0.20,0.26)</sub>	0.04 <sub>(0.03,0.07)</sub>
250	10	10.52 <sub>(9.08,12.25)</sub>	49.55 <sub>(37.79,62.85)</sub>	0.25 <sub>(0.22,0.26)</sub>	0.04 <sub>(0.03,0.05)</sub>
	15	10.64 <sub>(7.41,13.57)</sub>	48.93 <sub>(22.94,68.46)</sub>	0.25 <sub>(0.23,0.27)</sub>	0.04 <sub>(0.03,0.05)</sub>
	30	10.59 <sub>(7.41,13.57)</sub>	46.08 <sub>(22.95,69.46)</sub>	0.25 <sub>(0.23,0.27)</sub>	0.04 <sub>(0.03,0.05)</sub>
500	10	11.02 <sub>(9.74,12.69)</sub>	49.23 <sub>(39.56,60.36)</sub>	0.25 <sub>(0.23,0.27)</sub>	0.04 <sub>(0.03,0.04)</sub>
	15	11.41 <sub>(9.75,13.20)</sub>	48.42 <sub>(37.98,60.26)</sub>	0.25 <sub>(0.24,0.27)</sub>	0.04 <sub>(0.03,0.04)</sub>
	30	11.52 <sub>(9.72,13.61)</sub>	48.39 <sub>(36.61,62.35)</sub>	0.26 <sub>(0.24,0.28)</sub>	0.04 <sub>(0.03,0.04)</sub>

Table 6: Sensitivity analysis to the choice of the conditioning set size  $m$  and the mini-batch size  $n_B$ . Posterior mean and 95% credible intervals are displayed for each combination of  $n_B$  and  $m$ .

covariance parameters for SGRLD and NNGP. The posterior means and credible intervals for the range parameter  $\rho$ , and to a lesser extent the spatial variance  $\sigma^2$ , vary substantially between the two methods. The range estimates from SGRLD are almost three orders of magnitude higher than the NNGP estimate. Given the prediction results in Table 4, this indicates that the NNGP method is underestimating the range parameter. Furthermore, for NNGP, the credible interval for the range parameter has a total width of  $10^{-2}$ , perhaps indicating poor convergence. We also see from Table 5 that our SGRLD method allows fast exploration of the posterior and leads to almost 500 times more effective samples per unit time, while giving reasonable convergence (Figure 2).

Finally, as a sensitivity analysis, we compare the SGRLD results with mini-batch size  $n_B \in \{100, 250, 500\}$  and conditioning set size  $m \in \{10, 15, 30\}$ . Table 6 show the posterior mean and 95% credible intervals of the covariance parameters for all combinations of the two hyperparameters. The posterior mean of the spatial variance, smoothness and nugget vary little across these combinations of tuning parameters. For the range parameter, we notice a sensitivity to small batch sizes, *e.g.*,  $n_B = 100$  resulting in wide credible intervals and larger estimates compared to the other cases. For batch sizes  $\{250, 500\}$  the estimates are similar across values of  $m$ .



## 6 Discussion

SG methods offer considerable speed-ups when the data size is very large. In fact, one can take hundreds or even thousands of steps in one pass through the whole dataset in the time it takes for only one step if the full dataset is used. This enables fast exploration of the posterior in significantly less time. GPs however fall within the correlated setting case where SGMCMC methods have received limited attention. Spatial correlation is a critical component of GPs and naive subsampling during parameter estimation would lead to random divisions of the spatial domain at each iteration. By leveraging the form of the Vecchia approximation, we derive unbiased gradient estimates based on minibatches of the data. We developed a new stochastic gradient based MCMC algorithm for scalable Bayesian inference in large spatial data settings. Without the Vecchia approximation, subsampling strategies would always lead to biased gradient estimates. The proposed method also uses the exact Fisher information to speed up convergence and explore the parameter space efficiently. Our work contributes to the literature on scalable methods for Gaussian process, and can be extended to non Gaussian models *i.e.* classification.

## Acknowledgements

This research was partially supported by National Science Foundation grants DMS2152887 and DMR-2022254, and by grants from the Southeast National Synthesis Wildfire and the United States Geological Survey’s National Climate Adaptation Science Center (G21AC10045).

## References

- Aicher, C., Ma, Y.-A., Foti, N. J. and Fox, E. B. (2019) Stochastic gradient MCMC for state space models. *SIAM Journal on Mathematics of Data Science*, **1**, 555–587.
- Aicher, C., Putcha, S., Nemeth, C., Fearnhead, P. and Fox, E. B. (2021) Stochastic gradient MCMC for nonlinear state space models. *arXiv preprint arXiv:1901.10568*.
- Argo (2023) Argo Program Office. <https://argo.ucsd.edu/>. Accessed: 2023-11-26.
- Baker, J., Fearnhead, P., Fox, E. B. and Nemeth, C. (2019) Control variates for stochastic gradient MCMC. *Statistics and Computing*, **29**, 599–615.
- Banerjee, S., Gelfand, A. E., Finley, A. O. and Sang, H. (2008) Gaussian predictive process models for large spatial data sets. *Journal of the Royal Statistical Society: Series B (Statistical Methodology)*, **70**, 825–848.
- Barbian, M. H. and Assunção, R. M. (2017) Spatial subensemble estimator for large geostatistical data. *Spatial Statistics*, **22**, 68–88.
- Chee, J. and Toulis, P. (2018) Convergence diagnostics for stochastic gradient descent with constant learning rate. In *International Conference on Artificial Intelligence and Statistics*, 1476–1485. PMLR.
- Chen, C., Ding, N. and Carin, L. (2015) On the convergence of stochastic gradient MCMC algorithms with high-order integrators. In *Neural Information Processing Systems*. URL <https://api.semanticscholar.org/CorpusID:2196919>.
- Chen, H., Zheng, L., Al Kontar, R. and Raskutti, G. (2020) Stochastic gradient descent in correlated settings: A study on gaussian processes. *Advances in neural information processing systems*, **33**, 2722–2733.
- Chen, T., Fox, E. and Guestrin, C. (2014) Stochastic gradient Hamiltonian Monte Carlo. In *International conference on machine learning*, 1683–1691. PMLR.
- Cressie, N. (1988) Spatial prediction and ordinary kriging. *Mathematical geology*, **20**, 405–421.
- Cressie, N. and Johannesson, G. (2008) Fixed rank kriging for very large spatial data sets. *Journal of the Royal Statistical Society: Series B (Statistical Methodology)*, **70**, 209–226.
- Dalalyan, A. S. and Karagulyan, A. (2019) User-friendly guarantees for the Langevin Monte Carlo with inaccurate gradient. *Stochastic Processes and their Applications*, **129**, 5278–5311.
- Datta, A., Banerjee, S., Finley, A. O. and Gelfand, A. E. (2016) Hierarchical nearest-neighbor Gaussian process models for large geostatistical datasets. *Journal of the American Statistical Association*, **111**, 800–812.

- Dubey, K. A., J Reddi, S., Williamson, S. A., Póczos, B., Smola, A. J. and Xing, E. P. (2016) Variance reduction in stochastic gradient Langevin dynamics. *Advances in neural information processing systems*, **29**.
- Durmus, A. and Moulines, É. (2017) Nonasymptotic convergence analysis for the unadjusted Langevin algorithm. *The Annals of Applied Probability*, **27**, 1551 – 1587. URL<https://doi.org/10.1214/16-AAP1238>.
- Finley, A. O., Datta, A. and Banerjee, S. (2022) spNNGP R package for nearest neighbor Gaussian process models. *Journal of Statistical Software*, **103**, 1–40.
- Finley, A. O., Datta, A., Cook, B. D., Morton, D. C., Andersen, H. E. and Banerjee, S. (2019) Efficient algorithms for Bayesian nearest neighbor Gaussian processes. *Journal of Computational and Graphical Statistics*, **28**, 401–414.
- Furrer, R., Genton, M. G. and Nychka, D. (2006) Covariance tapering for interpolation of large spatial datasets. *Journal of Computational and Graphical Statistics*, **15**, 502–523.
- Gelfand, A. E. and Schliep, E. M. (2016) Spatial statistics and Gaussian processes: A beautiful marriage. *Spatial Statistics*, **18**, 86–104. URL<https://www.sciencedirect.com/science/article/pii/S2211675316300033>. Spatial Statistics Avignon: Emerging Patterns.
- Guhaniyogi, R. and Banerjee, S. (2018) Meta-kriging: Scalable Bayesian modeling and inference for massive spatial datasets. *Technometrics*.
- Guinness, J. (2018) Permutation and grouping methods for sharpening Gaussian process approximations. *Technometrics*, **60**, 415–429. URL<https://doi.org/10.1080/00401706.2018.1437476>. PMID: 31447491.
- (2019) Gaussian process learning via fisher scoring of vecchia’s approximation.
- Guinness, J., Katzfuss, M. and Fahmy, Y. (2018) Gpgp: fast Gaussian process computation using Vecchia’s approximation. *R package version 0.1. 0*.
- Hardt, M., Recht, B. and Singer, Y. (2016) Train faster, generalize better: Stability of stochastic gradient descent. In *International conference on machine learning*, 1225–1234. PMLR.
- Heaton, M. J., Datta, A., Finley, A. O., Furrer, R., Guinness, J., Guhaniyogi, R., Gerber, F., Gramacy, R. B., Hammerling, D., Katzfuss, M. et al. (2019) A case study competition among methods for analyzing large spatial data. *Journal of Agricultural, Biological and Environmental Statistics*, **24**, 398–425.
- Heaton, M. J. and Johnson, J. A. (2023) Minibatch Markov chain Monte Carlo algorithms for fitting Gaussian processes. *arXiv preprint arXiv:2310.17766*.

- Heidelberger, P. and Welch, P. D. (1981) A spectral method for confidence interval generation and run length control in simulations. *Communications of the ACM*, **24**, 233–245.
- Hinton, G., Srivastava, N. and Swersky, K. (2012) Neural networks for machine learning lecture 6a overview of mini-batch gradient descent. *Cited on*, **14**, 2.
- Kang, E., Liu, D. and Cressie, N. (2009) Statistical analysis of small-area data based on independence, spatial, non-hierarchical, and hierarchical models. *Computational Statistics & Data Analysis*, **53**, 3016–3032.
- Katzfuss, M. and Cressie, N. (2011) Spatio-temporal smoothing and em estimation for massive remote-sensing data sets. *Journal of Time Series Analysis*, **32**, 430–446.
- Katzfuss, M. and Guinness, J. (2021) A general framework for Vecchia approximations of Gaussian processes. *Statistical Science*, **36**, 124–141.
- Kaufman, C. G., Schervish, M. J. and Nychka, D. W. (2008) Covariance tapering for likelihood-based estimation in large spatial data sets. *Journal of the American Statistical Association*, **103**, 1545–1555.
- Kim, S., Song, Q. and Liang, F. (2022) Stochastic gradient Langevin dynamics with adaptive drifts. *Journal of statistical computation and simulation*, **92**, 318–336.
- Kingma, D. P. and Ba, J. (2014) Adam: A method for stochastic optimization. *arXiv preprint arXiv:1412.6980*.
- Li, C., Chen, C., Carlson, D. and Carin, L. (2016a) Preconditioned stochastic gradient Langevin dynamics for deep neural networks. In *Proceedings of the AAAI conference on artificial intelligence*, vol. 30.
- Li, W., Ahn, S. and Welling, M. (2016b) Scalable MCMC for mixed membership stochastic block-models. In *Artificial Intelligence and Statistics*, 723–731. PMLR.
- Ma, Y., Ma, Y.-A., Chen, T. and Fox, E. B. (2015) A complete recipe for stochastic gradient MCMC. In *Neural Information Processing Systems*. URL <https://api.semanticscholar.org/CorpusID:17950949>.
- Ma, Y.-A., Foti, N. J. and Fox, E. B. (2017) Stochastic gradient MCMC methods for hidden Markov models. In *International Conference on Machine Learning*, 2265–2274. PMLR.
- Mardia, K. V. and Marshall, R. J. (1984) Maximum likelihood estimation of models for residual covariance in spatial regression. *Biometrika*, **71**, 135–146. URL <http://www.jstor.org/stable/2336405>.
- Nemeth, C. and Fearnhead, P. (2021) Stochastic gradient Markov chain Monte Carlo. *Journal of the American Statistical Association*, **116**, 433–450. URL <https://doi.org/10.1080/01621459.2020.1847120>.

- Newton, D., Yousefian, F. and Pasupathy, R. (2018) Stochastic gradient descent: Recent trends. *Recent advances in optimization and modeling of contemporary problems*, 193–220.
- Robbins, H. and Monro, S. (1951) A Stochastic Approximation Method. *The Annals of Mathematical Statistics*, **22**, 400 – 407. URL<https://doi.org/10.1214/aoms/1177729586>.
- Roberts, G. O. and Rosenthal, J. S. (1998) Optimal scaling of discrete approximations to Langevin diffusions. *Journal of the Royal Statistical Society: Series B (Statistical Methodology)*, **60**. URL<https://api.semanticscholar.org/CorpusID:5831882>.
- Rue, H., Martino, S. and Chopin, N. (2009) Approximate Bayesian inference for latent Gaussian models by using integrated nested laplace approximations. *Journal of the Royal Statistical Society: Series B (Statistical Methodology)*, **71**, 319–392.
- Saha, S. and Bradley, J. R. (2023) Incorporating subsampling into Bayesian models for high-dimensional spatial data. *arXiv preprint arXiv:2305.13221*.
- Sang, H., Jun, M. and Huang, J. Z. (2011) Covariance approximation for large multivariate spatial data sets with an application to multiple climate model errors. *The Annals of Applied Statistics*, 2519–2548.
- Stein, M. L. (1999) *Interpolation of spatial data: some theory for kriging*. Springer Science & Business Media.
- (2002) The screening effect in Kriging. *The Annals of Statistics*, **30**, 298 – 323. URL<https://doi.org/10.1214/aos/1015362194>.
- (2011) 2010 Rietz lecture: When does the screening effect hold? *The Annals of Statistics*, **39**, 2795–2819. URL<http://www.jstor.org/stable/41713599>.
- Stein, M. L., Chi, Z. and Welty, L. J. (2004) Approximating likelihoods for large spatial data sets. *Journal of the Royal Statistical Society: Series B (Statistical Methodology)*, **66**, 275–296.
- Teh, Y., Thiéry, A. and Vollmer, S. (2016) Consistency and fluctuations for stochastic gradient Langevin dynamics. *Journal of Machine Learning Research*, **17**.
- Vecchia, A. V. (1988) Estimation and model identification for continuous spatial processes. *Journal of the Royal Statistical Society: Series B (Methodological)*, **50**, 297–312.
- Welling, M. and Teh, Y. W. (2011) Bayesian learning via stochastic gradient Langevin dynamics. In *International Conference on Machine Learning*. URL<https://api.semanticscholar.org/CorpusID:2178983>.
- Woodard, R. (2000) Interpolation of spatial data: some theory for kriging. *Technometrics*, **42**, 436.

## Appendix A.1: Computational Details

Here we give the detailed algorithms of the SG methods with adaptive drifts. The RMSprop (Root Mean Square Propagation) algorithm is an optimization algorithm originally developed for training neural networks models. It adapts the learning rates of each parameter based on the historical gradient information. This can be seen as adaptive preconditioning method.

---

**Algorithm 1: RMSprop Algorithm**

---

**Input:** Initial parameter values  $\theta_0$ , learning rate  $h_0$ , decay rate  $\rho$ , small constant  $\epsilon$

**Output:** Optimized parameter values  $\theta$

Initialize square gradient accumulator  $r_0 = 0$ ;

**while not converged do**

    Sample minibatch without repetition; Compute gradient  $\bar{g}$  on mini-batch;

    Accumulate squared gradient:  $r_t \leftarrow \rho r_{t-1} + (1 - \rho)\bar{g} \odot \bar{g}$ ;

    Update parameters:  $\theta_{t+1} \leftarrow \theta_t - h_t \bar{g} \oslash \sqrt{r_t + \epsilon}$ ;

---

Momentum SGD is an optimization algorithm that uses a Nesterov momentum term to accelerate the convergence in the presence of high curvature or noisy gradients. Momentum SGD proceeds as follows

---

**Algorithm 2: Momentum SGD Algorithm**

---

**Input:** Initial parameter values  $\theta_0$ , learning rate  $h_0$ , momentum term  $\alpha$

**Output:** Optimized parameter values  $\theta$

Initialize velocity  $v_0 = 0$ ;

**while not converged do**

    Sample minibatch without repetition; Compute gradient  $\bar{g}_t$  on mini-batch;

    Update velocity:  $v_t \leftarrow \alpha v_{t-1} - h_t \bar{g}_t$ ;

    Update parameters:  $\theta_{t+1} \leftarrow \theta_t + v_t$ ;

---

The Adam algorithm combines ideas from RMSprop and momentum to adaptively adjust learning rates.

---

**Algorithm 3:** Adam Algorithm

---

**Input:** Initial parameter values  $\theta_0$ , learning rate  $h_0$ , exponential decay rates for moments

$\alpha_1, \alpha_2$ , small constant  $\epsilon$

**Output:** Optimized parameter values  $\theta$

Initialize moment estimates  $m_0 = 0, v_0 = 0$ , time step  $t = 0$ ;

**while** *not converged* **do**

Sample minibatch without repetition; Compute gradient  $\bar{g}$  on mini-batch;

Update biased first moment estimate:  $m_{t+1} \leftarrow \alpha_1 m_t + (1 - \alpha_1) \bar{g}$ ;

Update biased second raw moment estimate:  $v_{t+1} \leftarrow \beta_2 v + (1 - \alpha_2) \bar{g} \odot \bar{g}$ ;

Correct bias in moment estimates:  $\hat{m}_t \leftarrow m_t / (1 - \alpha_1^t), \hat{v}_t \leftarrow v_t / (1 - \alpha_2^t)$ ;

Update parameters:  $\theta_{t+1} \leftarrow \theta_t - \alpha \hat{m}_t \odot (\sqrt{\hat{v}_t} + \epsilon)$ ;

---

## Appendix A.2: Additional Results

### Maximum likelihood estimates

As discussed in the simulation study section, a small modification to the SGRLD algorithm yields a stochastic Fisher scoring method for the likelihood using the Vecchia approximation. To perform Fisher scoring, we only need to remove the injected noise and drift terms from the updates in equations (13). Let  $\beta_t, \theta_t$  and  $h_t$ , the current values of the parameters and the step size respectively.

The SGFS scoring updates are

$$\beta_{t+1} = \beta_t + h_t p_{\mathcal{B}}^4(\theta_t)^{-1} (p_{\mathcal{B}}^3(\theta_t) - p_{\mathcal{B}}^4(\theta_t) \beta_t) \quad (34)$$

$$\theta_{t+1} = \theta_t + h_t \mathcal{I}_{\mathcal{B}}(\theta)^{-1} \nabla_{\theta_t} \bar{\ell}_{\mathcal{B}}(\beta_t, \theta_t), \quad (35)$$

where  $\mathcal{I}_B(\boldsymbol{\theta})$  is given in (31) and  $\nabla_{\boldsymbol{\theta}_t} \bar{\ell}_B(\boldsymbol{\beta}_t, \boldsymbol{\theta}_t)$  is the vector with elements defined in (30).

We compare the SGFS method to the full data Fisher scoring method in Guinness (2019) and the most widely used SGD variants. We limit the setting to  $N = 10^4$  locations, the learning rate scheduling and batch size dimensions are kept the same, and the number of epochs is set to 10. To avoid overfitting in the SGD methods we use the stopping rule proposed by Chee and Toulis (2018). This method keeps a running average of the inner product of successive gradients and detects when this quantity changes sign. The results are summarized in Table-7.

Table 7: Mean squared error of covariance parameters from  $10^4$  locations. Mean and standard deviation (in parenthesis) displayed over 100 simulations.

Algorithm	Variance	Range	Smoothness	Nugget	Time (in seconds)
<b>RMSPROP</b>	0.12(0.03)	0.39(0.069)	0.72(0.12)	$0.02(3 \cdot 10^{-4})$	9.26
<b>ADAM</b>	0.52(0.07)	0.69(0.02)	0.93(0.06)	$0.11(3 \cdot 10^{-3})$	11.71
<b>MSGD</b>	0.19(0.06)	0.48(0.10)	1.08(0.09)	$0.17(8 \cdot 10^{-3})$	10.05
<b>GpGp</b>	0.92(0.16)	0.09(0.02)	1.04(0.25)	$0.21(6 \cdot 10^{-3})$	38.72
<b>SGFS</b>	0.06(0.014)	0.10(0.04)	0.16(0.01)	$0.11(2 \cdot 10^{-2})$	14.03

The results in Table-7 show that the SGFS outperforms the other methods in terms of estimation error. Compared to GpGp, the stochastic methods take at most half the time while performing twenty times more iterations.